

Accepted Manuscript

Title: Tyrosinase biosensor based on a glassy carbon electrode modified with multi-walled carbon nanotubes and 1-butyl-3-methylimidazolium chloride within a dihexadecylphosphate film



Author: <ce:author id="aut0005" biographyid="vt0005"> Fernando Campanhã Vicentini<ce:author id="aut0010" biographyid="vt0010"> Bruno C. Janegitz<ce:author id="aut0015" biographyid="vt0015"> Christopher M.A. Brett<ce:author id="aut0020" biographyid="vt0020"> Orlando Fatibello-Filho

PII: S0925-4005(13)00914-3
DOI: <http://dx.doi.org/doi:10.1016/j.snb.2013.07.109>
Reference: SNB 15801

To appear in: *Sensors and Actuators B*

Received date: 19-5-2013
Revised date: 2-7-2013
Accepted date: 29-7-2013

Please cite this article as: F.C. Vicentini, B.C. Janegitz, C.M.A. Brett, O. Fatibello-Filho, Tyrosinase biosensor based on a glassy carbon electrode modified with multi-walled carbon nanotubes and 1-butyl-3-methylimidazolium chloride within a dihexadecylphosphate film, *Sensors and Actuators B: Chemical* (2013), <http://dx.doi.org/10.1016/j.snb.2013.07.109>

This is a PDF file of an unedited manuscript that has been accepted for publication. As a service to our customers we are providing this early version of the manuscript. The manuscript will undergo copyediting, typesetting, and review of the resulting proof before it is published in its final form. Please note that during the production process errors may be discovered which could affect the content, and all legal disclaimers that apply to the journal pertain.

Tyrosinase biosensor based on a glassy carbon electrode modified with multi-walled carbon nanotubes and 1-butyl-3-methylimidazolium chloride within a dihexadecylphosphate film

Fernando Campanhã Vicentini^a, Bruno C. Janegitz^{a,b}, Christopher M. A. Brett^c, Orlando Fatibello-Filho^{a,d,*}

^a *Departamento de Química, Centro de Ciências Exatas e de Tecnologia, Universidade Federal de São Carlos, Caixa postal 676, CEP 13560-970, São Carlos/SP, Brazil*

^b *Grupo de Biofísica Molecular Sérgio Mascarenhas, Instituto de Física de São Carlos, Universidade de São Paulo, CEP 13566-390, São Carlos/SP, Brazil*

^c *Departamento de Química, Faculdade de Ciências e Tecnologia, Universidade de Coimbra, 3004-535, Coimbra, Portugal*

^d *Instituto Nacional de Ciência e Tecnologia de Bioanalítica (INTC de Bioanalítica),*

Brazil

Corresponding author at: Departamento de Química, Universidade Federal de São Carlos, Caixa Postal 676, CEP 13560-970, São Carlos, SP, Brazil, Tel +55 16 33518098; FAX +55 16 33518350, E-mail address: bello@ufscar.br (Orlando Fatibello-Filho)

Abstract

A glassy carbon electrode modified with functionalized multi-walled carbon nanotubes (MWCNT), 1-butyl-3-methylimidazolium chloride (ionic liquid= IL) and tyrosinase (Tyr) within a dihexadecylphosphate (DHP) film for the development of a biosensor is proposed. MWCNT, IL and Tyr were efficiently immobilized in the film using 1-ethyl-3-(3-dimethylaminopropyl) carbodiimide/N-hydroxysuccinimide (EDC/NHS) as crosslinking agents, and which was characterized by cyclic voltammetry (CV) in the presence of catechol. The IL-MWCNT nanocomposite showed good conductivity and biocompatibility with Tyr enzyme, since the biosensor presented biocatalytic activity towards the oxidation of catechol to *o*-quinone which was electrochemically reduced to catechol at a potential of 0.04 V. The calibration curve ranged from 4.9×10^{-6} to 1.1×10^{-3} mol L⁻¹ with a detection limit of 5.8×10^{-7} mol L⁻¹. The developed Tyr-IL-MWCNT-DHP/GCE biosensor showed a wide linear range, good reproducibility, sensitivity and stability and the biosensor was successfully applied to the determination of catechol in natural water samples, with satisfactory results compared with a spectrophotometric method, at the 95% confidence level.

Keywords: 1-butyl-3-methylimidazolium chloride; Catechol determination; Dihexadecylphosphate; Ionic liquid; Multi-walled carbon nanotubes; Tyrosinase biosensor

1. Introduction

Room temperature ionic liquids (RTIL) are defined as compounds composed entirely of ions, which are liquid at a temperature less than 100 °C [1]. The use of ionic liquids in electroanalysis provides stability in the electrochemical responses and high ionic conductivity without the necessity of adding inert electrolyte. In recent years, RTILs have been used in the development of electrochemical sensors and biosensors, in most cases being incorporated in carbon paste [2] or carbon composite [3]. Nevertheless, there are very few biosensors using RTIL incorporated in film-modified electrodes. Film-modified electrodes are a good way to entrap proteins and enzymes, retaining their bioactivity whilst not interfering in the electrochemical response.

Carbon nanotubes (CNTs) present similarity in length scales with redox enzymes, they have high electronic conductivity and good mechanical properties, which can improve biosensing devices [4-7], such as tyrosinase biosensors. Ozoner et al. proposed a flow injection catechol biosensor based on tyrosinase entrapped in a CNT-modified polypyrrole biocomposite film on a glassy carbon electrode substrate [8]. Man and Yo prepared a biosensor containing tyrosinase, single-walled CNT and polypyrrole for amperometric detection of dopamine [9]. Tsai and Chiu developed an amperometric biosensor based on multi-walled CNT-Nafion-tyrosinase nanobiocomposites for the determination of phenolic compounds [10].

Dihexadecylphosphate (DHP), or dicetylphosphate, is a surfactant molecule with a polar head and two long hydrophobic tails [11]. It can produce stable films on electrode surfaces, probably via hydrogen bonds, and has been used in sensors [12] and biosensors [13].

Tyrosinase (Tyr) is a blue copper protein (with 2 copper atoms in the active centre), which can be considered as a polyphenol oxidase (PPO). This important enzyme catalyzes two consecutive oxidation reactions: 1) the *o*-hydroxylation of phenols to guaiacol and subsequently, 2) the oxidation of guaiacol to *o*-quinones, both in the presence of molecular oxygen. Furthermore, Tyr has been extensively used in biosensor construction for the determination of phenols [14, 15]. Janegitz and co-workers proposed a new phenol biosensor based on direct electron transfer by immobilizing Tyr on AuNPs electrodeposited on the surface of a BDD electrode [16]. In other work, Yang and co-workers constructed a novel nanocomposite film of tyrosinase–chitosan–carbon-coated nickel nanoparticles (CNi) for the detection of catechol [17]. Arecchi and co-workers developed a tyrosinase-modified amperometric biosensor for the detection of phenolic compounds in food, in which the enzyme was immobilized by drop-coating on a glassy carbon electrode covered by a polyamidic nanofibrous membrane prepared by electrospinning [18].

The aim of this work is to evaluate the advantages of a new catechol biosensor using 1-butyl-3-methylimidazolium chloride ionic liquid (IL) immobilised within a dihexadecylphosphate (DHP) film containing functionalized multi-walled carbon nanotubes (MWCNT) and tyrosinase (Tyr) enzyme.

2. Experimental

2.1 Reagents and solutions

Tyrosinase 50 kU (from mushroom) and dihexadecylphosphate were purchased from Sigma. MWCNT (20-30 nm in diameter, 1-2 nm wall thickness and 0.5–2 μm in length and 95% purity), 1-(3-dimethyl-aminopropyl)-3-ethylcarbodiimide hydrochloride (98%), 1-butyl-3-methylimidazolium chloride, N-hydroxysuccinimide (98%) were purchased from Aldrich. Catechol (99 %) and 4-aminoantipyrine were purchased from Sigma-Aldrich. All other chemicals were of analytical grade.

A 0.01 mol L⁻¹ catechol stock solution was prepared in a 0.1 mol L⁻¹ phosphate buffer solution (pH 7.0), which was made using NaH₂PO₄ and Na₂HPO₄. All solutions were prepared with Millipore Milli-Q nanopure water (resistivity > 18 M Ω cm). The phosphate buffer solution was employed as the supporting electrolyte in all the measurements with the biosensor.

2.2 Apparatus

The voltammetric experiments were conducted with a three-electrode system: the biosensor Tyr-IL-MWCNT-DHP/GCE as working electrode, a platinum wire as counter electrode, and Ag/AgCl (3.0 mol L⁻¹ KCl) as reference electrode, to which all potentials are referred. Voltammetric measurements were carried out using a model PGSTAT12 potentiostat/galvanostat (Metrohm-Autolab, Utrecht, Netherlands) controlled by GPES 4.9 software. Cyclic and linear voltammetric measurements were carried out in a 20.0 mL electrochemical cell. The background current was subtracted from all voltammograms. All experiments were carried out at room temperature.

A Supra 35-VP equipment (Carl Zeiss, Germany) with electron beam energy of 25 keV, was used to obtain the FEG-SEM images.

Measurements of pH were performed using an Orion pH-meter, Expandable Ion Analyser, model EA-940, connected to a Digimed combined glass electrode with an external Ag/AgCl (3.0 mol L^{-1} KCl) reference electrode.

For comparison, a spectrophotometric method for catechol determination [19] was carried out using a Femto spectrophotometer (model 435, Brazil) with a quartz cuvette (optical path length of 10 mm).

2.3. Functionalization of the multi-walled carbon nanotubes (acid treatment)

The MWCNT were initially purified with 2.0 mol L^{-1} HCl solution to remove metallic impurities, and were then submitted to a chemical pre-treatment using a mixture of concentrated nitric and sulfuric acids 3:1 (v/v) for 12 h at room temperature. After this, the suspension was centrifuged, the solid was washed several times with ultrapure water until pH 6.5–7.0 and was then dried at $120 \text{ }^\circ\text{C}$ for 6 h. The acid treatment promotes the appearance of polar hydrophilic surface groups, such as carboxyl ($-\text{COOH}$), hydroxyl ($-\text{OH}$), quinone ($-\text{C}(\text{=O})$), nitro ($-\text{NO}_2$), and amino groups ($-\text{NH}_2$) at the ends or at the sidewall defects of the nanotube structure [20-22]. After the acid treatment of MWCNT, an increase in the amount of carboxylic groups occurs, as described in detail in a previous, recent article [7].

2.4 Preparation of the Tyr-IL-MWCNT-DHP/GCE biosensor

A glassy carbon electrode (GCE, 5 mm diameter) was carefully polished to a mirror finish with 0.3 and $0.05 \text{ }\mu\text{m}$ alumina slurries, and rinsed thoroughly with Milli-Q water. The GCE was sonicated in isopropyl alcohol and then with Milli-Q water, each for about 5 min, and dried at room temperature.

A mass of 1.0 mg of MWCNT and 1.0 mg of DHP was added to 700 μL of 0.1 mol L^{-1} phosphate buffer solution (pH 7.0) and subjected to ultrasonication for 30 min to give a MWCNT-DHP suspension and then, 100 μL of 50 mg mL^{-1} IL solution in 0.1 mol L^{-1} phosphate buffer solution was added and the mixture ultrasonicated for a further 30 min. Afterwards, an aliquot of 200 μL of solution containing 1.0×10^{-3} mol L^{-1} 1-ethyl-3-(3-dimethylaminopropyl) carbodiimide (EDC) and 2.0×10^{-2} mol L^{-1} N-hydroxysuccinimide (NHS) was added in suspension for the carboxyl coupling reaction, carried out for 2 h with magnetic stirring. A mass of 1.20 mg enzyme (2000 U Tyr) was added to the MWCNT suspension and stirred for 2 h. During mixing, Tyr molecules were linked by covalent bond formation between the $-\text{COOH}$ groups of the MWCNT and $-\text{NH}_2$ of the enzyme [23]. Finally, a stable black suspension was obtained containing 1.0 mg of MWCNT, 1.0 mg of DHP and 5.0 mg of IL per mL. Subsequently, 20 μL of this suspension was cast onto the surface of a GCE and the solvent allowed to evaporate at 25 ± 1 $^\circ\text{C}$ for 12 h. Fig. 1 shows the biosensor fabrication process.

The Tyr-IL-MWCNT-DHP/GCE biosensor was stored at 4 $^\circ\text{C}$ in a refrigerator in 0.1 mol L^{-1} phosphate buffer solution (pH 7.0), when not in use.

Insert Fig. 1 here

2.5 Preparation of water samples

Natural water samples, A, B and C, were collected from a lake at São Carlos Federal University (São Carlos city - Brazil) (GPS A = $21^\circ 59' 09.47''\text{S}$ $47^\circ 52' 56.07''\text{W}$, B = $21^\circ 59' 10.45''\text{S}$ $47^\circ 52' 55.31''\text{W}$ and C = $21^\circ 59' 07.53''\text{S}$ $47^\circ 52' 51.01''\text{W}$). A sample of tap water, D, was collected at the same university. A fixed volume (25 mL) was transferred to four different calibration flasks (50 mL). After this, an aliquot of 5.0 mL of a 1.0×10^{-2} mol L^{-1} catechol standard solution was

carefully added to each and the final volume of 50 mL reached by addition of ultrapure water. The samples were stirred in order to homogenize the solutions. All solutions were used without any pre-treatment and were freshly prepared just before the measurements.

2.6. Spectrophotometric comparison method

A spectrophotometric method [19] was employed in order to compare the results obtained with the proposed voltammetric method. This method involves the construction of an analytical curve by monitoring the amount of antipyrine dye formed by the reaction of 4-aminoantipyrine and catechol. The blank, samples and standards were treated as follows. An accurate volume (100 mL) was transferred into a 250 mL beaker together with 2.5 mL of a 0.5 mol L⁻¹ NH₃ solution, and the pH was adjusted to 7.9 with phosphate buffer solution. Then, 1.0 mL of a 20.0 g L⁻¹ 4-aminoantipyrine solution was added and mixed well, followed by 1.0 mL of a 80.0 g L⁻¹ K₃Fe(CN)₆ solution. After 15 min, absorbances (blank, samples and standards) were measured at 500 nm.

3. Results and discussion

3.1 Characteristics of the IL-MWCNT-DHP/GCE electrode

The IL-MWCNT-DHP/GCE electrodes were characterised electrochemically. The combination of functionalized MWCNT and IL results in a nanocomposite with good conductivity and biocompatibility. In addition, the proposed film can increase the electrode electroactive area, as shown below.

The electroactive area of GCE, DHP/GCE, IL-DHP/GCE, MWCNT-DHP/GCE and IL-MWCNT-DHP/GCE was estimated in 0.1 mol L⁻¹ KCl solution in the presence of 1.0 × 10⁻³ mol L⁻¹ potassium hexacyanoferrate (II) (data not shown), applying the Randles–Sevcik equation [24]:

$$I_{pa} = 2.69 \times 10^5 n^{3/2} A D^{1/2} C v^{1/2} \quad \text{Eq. 1}$$

where I_{pa} is the anodic peak current (A), n is the number of electrons transferred, A is the electroactive area (cm²), D is the diffusion coefficient of [Fe(CN)₆]⁴⁻ in 0.1 mol L⁻¹ KCl solution (6.2 × 10⁻⁶ cm² s⁻¹), v is the potential scan rate (V s⁻¹), and C is the [Fe(CN)₆]⁴⁻ concentration in bulk solution (mol cm⁻³). The slopes of I_{pa} vs. $v^{1/2}$ plots for the oxidation process (data not shown) were: 4.77 × 10⁻⁵, 2.29 × 10⁻⁵, 3.11 × 10⁻⁵, 7.44 × 10⁻⁵ and 11.0 × 10⁻⁵ A V^{-1/2} s^{1/2} for GCE, DHP/GCE, IL-DHP/GCE, MWCNT-DHP/GCE and IL-MWCNT-DHP/GCE, respectively. The estimated electroactive areas were thus 0.071 cm², 0.034 cm², 0.046 cm², 0.11 cm² and 0.16 cm² for GCE, DHP/GCE, IL-DHP/GCE, MWCNT-DHP/GCE and IL-MWCNT-DHP/GCE, respectively. The combination of MWCNT and IL increased the electroactive surface area by a factor of 2.3 compared to the GCE. This increase can be attributed to the unfolding of MWCNT promoted by IL through ‘cation-π’ interactions between the imidazolium cation of the IL and the π-electrons of the MWCNT surface, increasing the number of exposed MWCNT electroactive sites [25-27].

The influence of IL concentration from 3.0 to 10 mg mL⁻¹ in the film, at a fixed amount of MWCNT in DHP 1.0 mg mL⁻¹, on the analytical signal was also investigated. For this purpose, a 1.0 × 10⁻³ mol L⁻¹ [Fe(CN)₆]⁴⁻ in 0.1 mol L⁻¹ KCl solution and potential scan rate of 100 mV s⁻¹ were used. The peak current increased with the increase of IL concentration up to 5.0 mg mL⁻¹ in the film (see Fig. SD-1 in the

supplementary data). When the concentration of IL was higher than 5.0 mg mL^{-1} the peak current decreased significantly. Thus, a 5.0 mg mL^{-1} IL concentration was selected for further studies.

3.2 Characterisation of the Tyr-IL-MWCNT-DHP/GCE biosensor

3.2.1 Scanning electron microscopy

Fig. 2 shows scanning electron microscopy (SEM) images of IL-MWCNT-DHP and Tyr-IL-MWCNT-DHP on the surface of GCE. Initially, before enzyme immobilization, Fig.2A, it can be seen that the MWCNT are uniformly distributed in the IL-MWCNT-DHP nanocomposite film. Tyr was then immobilized within the IL-MWCNT-DHP film by using EDC and NHS crosslinking agents that link the MWCNT carboxylic to the amine groups, as described previously [13]. After Tyr is immobilized (Fig. 2B), the surface morphology shows agglomerates that can be attributed to enzyme on the surface of the CNTs.

Insert Fig. 2 here

3.2.2 Electrochemical behaviour of catechol

The electrochemical behaviour of the catechol system was evaluated using the proposed biosensor. Fig. 3 shows cyclic voltammograms (CVs) obtained for Tyr-MWCNT-DHP/GCE and Tyr-IL-MWCNT-DHP/GCE biosensors, after thirty cycles in 0.1 mol L^{-1} phosphate buffer solution (pH 7) containing $1.0 \times 10^{-4} \text{ mol L}^{-1}$ catechol at a scan rate of 100 mV s^{-1} . As can be observed, the presence of IL in the biosensor leads to a considerable increase in the current response. Under the same conditions, the Tyr-IL-MWCNT-DHP/GCE (Fig. 3B, solid line) gives higher anodic and cathodic current peaks than the biosensor without IL (Fig. 3A, dashed line). Thus, the cathodic peak

current increased from $-3.8 \mu\text{A}$ at Tyr-MWCNT-DHP/GCE to $-7.6 \mu\text{A}$ at Tyr-IL-MWCNT-DHP/GCE and the anodic peak current from $2.9 \mu\text{A}$ to $7.7 \mu\text{A}$ for the biosensor containing IL. In the absence of Tyr in the modified electrode, the CVs are similar but the oxidation and reduction current response is lower by about 30 %, since no additional effect from enzymatic conversion of catechol to *o*-quinone (which can be reduced and then reoxidised) can occur.

The Tyr-IL-MWCNT-DHP/GCE biosensor presented well-defined anodic and cathodic peaks of similar magnitude and nearly symmetric at 0.300 and 0.040 V (scan rate 100 mV s^{-1}), respectively, with an I_{pa}/I_{pc} ratio equal to one, a formal potential, E° , of 170 mV and peak separation (ΔE_p) of 260 mV. The presence of IL in the biosensor, showed an improvement in the reversibility of the system when compared with the biosensor in the absence of IL which presented a ΔE_p of 383 mV.

Insert Fig. 3 here

These results show a synergic effect due the coupling of IL and MWCNT, which combines the high conductivity of ionic liquid with the electrocatalytic activity and/or increase of the analytical signal by the MWCNT.

The effect of scan rate on the analytical response of the Tyr-IL-MWCNT-DHP/GCE biosensor was evaluated for a $1.0 \times 10^{-4} \text{ mol L}^{-1}$ catechol solution in 0.1 mol L^{-1} phosphate buffer solution (pH 7.0). There was a shift in the peak potentials and increase in peak-to-peak separation with increasing scan rate, as can be seen in Fig. SD-2 in the supplementary data. The linear dependence of the anodic and cathodic peak currents with scan rate in the range 10 to 500 mV s^{-1} indicates that the process is controlled by the redox monolayer containing the immobilised Tyr and might be treated using Laviron's equations [28]:

$$E_{pc} = E^{\circ} + \frac{2.3RT}{\alpha nF} \left\{ \log \frac{\alpha nF}{RTk_s} + \log v \right\} \quad \text{Eq. 2}$$

$$E_{pa} = E^{\circ} - \frac{2.3RT}{(1-\alpha)nF} \left\{ \log \frac{(1-\alpha)nF}{RTk_s} + \log v \right\} \quad \text{Eq. 3}$$

$$\Delta E_p = \frac{2.3RT}{\alpha(1-\alpha)nF} \left\{ \alpha \log(1-\alpha) + (1-\alpha) \log \alpha - \log \frac{RTk_s}{nF} + \log v \right\} \quad \text{Eq. 4}$$

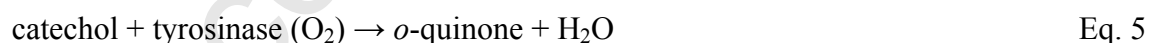
where E_{pa} and E_{pc} are the anodic and cathodic peak potentials, respectively, $\Delta E_p = E_{pa} - E_{pc}$, α is the charge transfer coefficient, v is the potential scan rate (V s^{-1}), k_s is the heterogeneous electron transfer rate constant (s^{-1}), R is the ideal gas constant ($8.314 \text{ J mol}^{-1} \text{ K}^{-1}$), F is the Faraday constant ($96,485 \text{ C mol}^{-1}$) and T is the temperature in Kelvin (298.15 K).

From the slopes of the plot of the anodic and cathodic peak potentials versus the logarithm of the potential scan rate (see Fig. SD-3 in the supplementary data, insert), the value of $\alpha_a n$ was calculated to be 0.92 and $\alpha_c n = 1.08$, which strongly suggests that $n = 2$, verified below. The value of k_s was calculated to be $35.1 \pm 0.8 \text{ s}^{-1}$ from a plot of ΔE_p versus the logarithm of the potential scan rate (see Fig. SD-3). This value is almost ten times higher than that previously reported by Wang et al [29] at a poly(diallyldimethylammonium chloride) functionalized graphene-modified glassy carbon electrode (3.85 s^{-1}). The high value obtained indicates the great ability of the proposed biosensor to promote electron transfer between *o*-quinone and the electrode surface and can be attributed to the structure of MWCNT that have a large number of defects as well as the synergistic effect of MWCNT and IL in promoting *o*-quinone electrocatalysis.

3.2.3 Influence of pH on the determination of catechol

The influence of pH on the cathodic peak current of the Tyr-IL-MWCNT-DHP/GCE biosensor was evaluated in the presence of 1.0×10^{-4} mol L⁻¹ catechol solution in a 0.1 mol L⁻¹ phosphate buffer solution at scan rate 100 mV s⁻¹. Since the literature reports that free Tyr loses activity irreversibly below pH 4.5 and above pH 9.3 [30-32], the selected pH range was from 5.5 to 8.0. The cathodic peak currents increased with increase in pH up to 7.0, as seen in Fig. 4A (insert). Above pH 7.0 the peak currents decreased. Therefore, phosphate buffer solution at pH 7.0 was selected as the supporting electrolyte for further studies.

The effect of solution pH on the anodic and cathodic peak potentials of Tyr-IL-MWCNT-DHP/GCE was also evaluated. As can be seen in Fig. 4, an increase of pH leads to a negative shift in both peak potentials. Fig. 4B (insert) shows a plot of the formal potential ($E^{\circ'} = (E_{pa} + E_{pc}) / 2$) versus pH. In this study, the formal potential showed a linear dependence with buffer pH following the equation $E^{\circ'} \text{ (V)} = 0.554 - 0.054 \text{ pH}$ with a correlation coefficient of 0.996. The value of the slope was -54 mV pH^{-1} , which was close to the theoretical value (59.2 mV pH^{-1}) at 25 °C for a reversible process involving equal numbers of protons and electrons [35, 36] and, according to Equation 6, the enzymatically produced *o*-quinone (Eq. 5) is electrochemically reduced to catechol at the electrode surface.



A schematic representation of the electrode process is shown in Fig. 5.

Insert Fig. 4 here

Insert Fig. 5 here

3.3. Determination of catechol by linear sweep voltammetry

The dependence of the cathodic peak current for reduction of *o*-quinone to catechol on LSV scan rate was evaluated in the range from 10 to 150 mV s⁻¹ in the presence of 5.0×10^{-5} mol L⁻¹ catechol solution in a 0.1 mol L⁻¹ phosphate buffer solution (pH 7.0). A linear increase in the magnitude of the peak current with increase of scan rate was observed up to 100 mV s⁻¹. Thus, this scan rate was chosen for construction of the analytical curve. Fig. 6 shows voltammograms obtained and the analytical curve (insert) for catechol using the proposed Tyr-IL-MWCNT-DHP/GCE biosensor.

The LSV method showed a linear response to catechol in the concentration range from 4.9×10^{-6} to 1.1×10^{-3} mol L⁻¹, following the equation $\Delta I_{pc} (\mu A) = 0.69 + 3.28 \times 10^4 C$ (mol L⁻¹) with a correlation coefficient of 0.998. The limit of detection (three times the standard deviation for the blank solution (n=10) divided by the slope of the analytical curve) was calculated as 5.8×10^{-7} mol L⁻¹.

Insert Fig. 6 here

Insert Table 1 here

The analytical figures of merit of the proposed method were compared with those reported in the literature, Table 1. It can be seen that the proposed Tyr-IL-MWCNT-DHP/GCE biosensor has a wide linear range (almost three decades), which was greater than those reported for other catechol sensors [6, 8, 15, 32, 35-42]. It presents a limit of detection lower than the biosensors in [8, 15, 35-37, 39-41] and higher than biosensors [6, 32, 38, 42]. The sensitivity of the proposed voltammetric method is higher than those of [8, 36, 38, 41] and lower than those of [6, 15, 40]. In addition, the proposed biosensor exhibited a great stability, assigned to the biocompatibility of Tyr-IL-MWCNT.

The apparent Michaelis–Menten kinetic constant (K_M^{app}) provides important information about the catalytic activity and affinity between enzyme and substrate. It can be estimated from the Lineweaver-Burk equation (double reciprocal plot) [16, 39]:

$$\frac{1}{I_s} = \frac{1}{I_{\text{máx}}} + \frac{K_M^{\text{app}}}{I_{\text{máx}}} \frac{1}{[\text{catechol}]} \quad \text{Eq. 7}$$

where I_s is the steady-state current measured for enzymatic product and $I_{\text{máx}}$, is the maximum current under condition of substrate (catechol) saturation.

The equation of the Lineweaver-Burk plots for the Tyr-IL-MWCNT-DHP/GCE biosensor was $1/I_s = 0,203 + 38.61 \times 1/[\text{catechol}]$ (correlation coefficient of 0.995). Table 2 presents K_M^{app} values reported in the literature for different tyrosinase biosensors using catechol as substrate. The $I_{\text{máx}}$ and K_M^{app} values obtained in this work were 4.93×10^{-6} A and 1.9×10^{-4} mol L⁻¹ respectively, which is in agreement with the values previously reported for a biosensor containing MWCNT and magnetic nanoparticles [41], self-assembled monolayers in a gold electrode [43], a graphite electrode [44] and a reticulated vitreous carbon–epoxy resin [45]. Higher values of K_M^{app} than in this work were reported by Campuzano et al. [46] for Tyr immobilized on self-assembled monolayers, by Kiralp et al. [47] for Tyr immobilized on polypyrrole and the reports for free Tyr [47-50]. This suggests that the enzyme immobilized in IL-MWCNT, has a high catalytic activity with a high affinity for catechol, owing to an increase of the electron transfer rate.

Insert Table 2 here

3.4. Determination of catechol in water samples using the Tyr-IL-MWCNT-DHP/GCE biosensor

The Tyr-IL-MWCNT-DHP/GCE biosensor was applied to the determination of the concentration of catechol in four water samples (three natural water samples, A – C, and one tap water sample, D, using the standard addition method. As catechol was not found in the samples, aliquots of 100 μL of fortified samples (procedure described previously) were added to the electrochemical cell containing 20 mL of 0.1 mol L^{-1} phosphate buffer solution (pH 7.0) to obtain a 5.0×10^{-5} mol L^{-1} catechol concentration. For each sample three determinations were done, and the standard deviations were calculated. Table 3 presents the concentrations of catechol determined in water samples employing the proposed LSV method and the spectrophotometric method [19]. After applying the paired t-test [51] to the results obtained by both methods, the calculated t value of 2.468 is smaller than the critical value (3.182, $\alpha = 0.05$), so one may conclude that there is no difference between the two methods at a confidence level of 95%. This demonstrates that the Tyr-IL-MWCNT-DHP/GCE biosensor is appropriate for the determination of catechol in water samples. Other advantages are ease of preparation, relatively low cost, stability and lifetime.

Insert Table 3 here

The repeatability ($n=10$) of one Tyr-IL-MWCNT-DHP/GCE biosensor was evaluated in a 5.0×10^{-5} mol L^{-1} catechol solution. The relative standard deviation (RSD) values obtained for intra-day repeatability was 1.16% and inter-day repeatability was 2.94%, indicating a good stability of the film. Furthermore, the reproducibility of the method was determined from the response of five different Tyr-IL-MWCNT-DHP/GCE biosensors in the presence of 5.0×10^{-5} mol L^{-1} catechol. A relative standard deviation of 4.86% was obtained, indicating high reproducibility.

The long-term stability of the Tyr-IL-MWCNT-DHP/GCE biosensor was evaluated by monitoring the response in the presence of 1.0×10^{-5} mol L^{-1} catechol in

0.1 mol L⁻¹ phosphate buffer solution (pH 7.0) during 30 days (190 determinations in this period). The cathodic current response decreased by only 5.0 % after this time. This stability is due to two main factors, the immobilization procedure, which provides good entrapment of the enzyme within the IL-MWCNT-DHP film and to the biocompatibility between MWCNT and Tyr.

The interference of species such as sodium, potassium, magnesium, calcium, aluminum, iron(III) cations and carbonate, chloride, phosphate and sulfate anions and humic acid on catechol determination was evaluated in phosphate buffer solution (pH 7.0) containing 5.0×10^{-5} mol L⁻¹ catechol spiked concomitantly with each interferent (5.0×10^{-3} mol L⁻¹). The results showed that for all tested species a change in the electrode response of less than 5 % occurred and did not disrupt the determination of catechol by the proposed biosensor at the concentration evaluated.

4. Conclusions

In this study, the enzyme tyrosinase was successfully immobilized in IL-MWCNT-DHP/GCE. The use of MWCNT and IL, led to a synergistic effect by combining the high conductivity and biocompatibility of the ionic liquid with the MWCNT electrocatalytic activity and increased analytical signal. The Tyr-IL-MWCNT-DHP/GCE biosensor was applied to the determination of catechol by LSV with linear responses in the concentration range from 4.9×10^{-6} to 1.1×10^{-3} mol L⁻¹ and a detection limit of 5.8×10^{-7} mol L⁻¹, besides presenting good intra and inter-day repeatability. The Tyr-IL-MWCNT-DHP/GCE biosensor was applied to the determination of catechol in water samples with good results, exhibiting high stability and long lifetime. Moreover, the use of this biosensor architecture can be an excellent methodology to immobilize other enzymes or proteins.

Acknowledgements

The authors gratefully acknowledge Conselho Nacional de Desenvolvimento Científico e Tecnológico (CNPq), Coordenação de Aperfeiçoamento de Pessoal de Nível Superior (CAPES), Instituto Nacional de Ciência e Tecnologia de Bioanalítica (INCTBio), and Fundação de Amparo à Pesquisa do Estado de São Paulo (FAPESP), for financial support and scholarships. We also thank Fundação para a Ciência e a Tecnologia (FCT), Portugal PTDC/QUI-QUI/116091/2009, POCH, POFC-QREN (co-financed by FSE and European Community FEDER funds through the program COMPETE and FCT project PEst-C/EME/UI0285/2013.

References

- [1] M.J.A. Shiddiky, A.A.J. Torriero, Application of ionic liquids in electrochemical sensing systems, *Biosens. Bioelectron.*, 26 (2011) 1775-1787.
- [2] K.D. Maguerroski, S.C. Fernandes, A.C. Franzoi, I.C. Vieira, Pine nut peroxidase immobilized on chitosan crosslinked with citrate and ionic liquid used in the construction of a biosensor, *Enzyme Microb. Technol.*, 44 (2009) 400-405.
- [3] M.M. Musameh, R.T. Kachosangi, L. Xiao, A. Russell, R.G. Compton, Ionic liquid-carbon composite glucose biosensor, *Biosens. Bioelectron.*, 24 (2008) 87-92.
- [4] E.R. Sartori, F.C. Vicentini, O. Fatibello-Filho, Indirect determination of sulfite using a polyphenol oxidase biosensor based on a glassy carbon electrode modified with multi-walled carbon nanotubes and gold nanoparticles within a poly(allylamine hydrochloride) film, *Talanta*, 87 (2011) 235-242.
- [5] B.C. Janegitz, L.C.S. Figueiredo-Filho, L.H. Marcolino-Junior, S.P.N. Souza, E.R. Pereira-Filho, O. Fatibello-Filho, Development of a carbon nanotubes paste electrode modified with crosslinked chitosan for cadmium(II) and mercury(II) determination, *J. Electroanal. Chem.*, 660 (2011) 209-216.
- [6] J. Ren, T.F. Kang, R. Xue, C.N. Ge, S.Y. Cheng, Biosensor based on a glassy carbon electrode modified with tyrosinase immobilized on multiwalled carbon nanotubes, *Microchim. Acta*, 174 (2011) 303-309.
- [7] B.C. Janegitz, L.H. Marcolino-Junior, S.P. Campana, R.C. Faria, O. Fatibello-Filho, Anodic stripping voltammetric determination of copper(II) using a functionalized carbon nanotubes paste electrode modified with crosslinked chitosan, *Sens. Actuator B-Chem.*, 142 (2009) 260-266.
- [8] S.K. Ozoner, M. Yalvac, E. Erhan, Flow injection determination of catechol based on polypyrrole-carbon nanotube-tyrosinase biocomposite detector, *Curr. Appl. Phys.*, 10 (2010) 323-328.
- [9] K. Min, Y.J. Yoo, Amperometric detection of dopamine based on tyrosinase-SWNTs-Ppy composite electrode, *Talanta*, 80 (2009) 1007-1011.
- [10] Y.C. Tsai, C.C. Chiu, Amperometric biosensors based on multiwalled carbon nanotube-Nafion-tyrosinase nanobiocomposites for the determination of phenolic compounds, *Sens. Actuator B-Chem.*, 125 (2007) 10-16.
- [11] Y. Wu, Nano-TiO₂/dihexadecylphosphate based electrochemical sensor for sensitive determination of pentachlorophenol, *Sensors and Actuators B: Chemical*, 137 (2009) 180-184.
- [12] S.J. Yao, J.H. Xu, Y. Wang, X.X. Chen, Y.X. Xu, S.S. Hu, A highly sensitive hydrogen peroxide amperometric sensor based on MnO₂ nanoparticles and dihexadecyl hydrogen phosphate composite film, *Anal. Chim. Acta*, 557 (2006) 78-84.
- [13] B.C. Janegitz, R. Pauliukaite, M.E. Ghica, C.M.A. Brett, O. Fatibello-Filho, Direct electron transfer of glucose oxidase at glassy carbon electrode modified with functionalized carbon nanotubes within a dihexadecylphosphate film, *Sens. Actuator B-Chem.*, 158 (2011) 411-417.
- [14] D. Fiorentino, A. Gallone, D. Fiocco, G. Palazzo, A. Mallardi, Mushroom tyrosinase in polyelectrolyte multilayers as an optical biosensor for o-diphenols, *Biosens. Bioelectron.*, 25 (2010) 2033-2037.
- [15] C. Apetrei, M.L. Rodriguez-Mendez, J.A. De Saja, Amperometric tyrosinase based biosensor using an electropolymerized phosphate-doped polypyrrole film as an

- immobilization support. Application for detection of phenolic compounds, *Electrochim. Acta*, 56 (2011) 8919-8925.
- [16] B.C. Janegitz, R.A. Medeiros, R.C. Rocha-Filho, O. Fatibello-Filho, Direct electrochemistry of tyrosinase and biosensing for phenol based on gold nanoparticles electrodeposited on a boron-doped diamond electrode, *Diam. Relat. Mat.*, 25 (2012) 128-133.
- [17] L. Yang, H. Xiong, X. Zhang, S. Wang, A novel tyrosinase biosensor based on chitosan-carbon-coated nickel nanocomposite film, *Bioelectrochemistry*, 84 (2012) 44-48.
- [18] A. Arecchi, M. Scampicchio, S. Drusch, S. Mannino, Nanofibrous membrane based tyrosinase-biosensor for the detection of phenolic compounds, *Anal. Chim. Acta*, 659 (2010) 133-136.
- [19] A.E. Greenberg, L.S. Clesceri, A.D. Eaton, *Standard Methods for the Examination of Water and Wastewater*, 19th ed., American Public Health Association, USA, 1995.
- [20] X. Jiang, J. Gu, X. Bai, L. Lin, Y. Zhang, The influence of acid treatment on multi-walled carbon nanotubes, *Pigm. Resin. Technol.*, 38 (2009) 165-173.
- [21] Y. Shirazi, M.A. Tofiqhy, T. Mohammadi, A. Pak, Effects of different carbon precursors on synthesis of multiwall carbon nanotubes: Purification and Functionalization, *Appl. Surf. Sci.*, 257 (2011) 7359-7367.
- [22] L. Wang, S.A. Feng, J.H. Zhao, J.F. Zheng, Z.J. Wang, L. Li, Z.P. Zhu, A facile method to modify carbon nanotubes with nitro/amino groups, *Appl. Surf. Sci.*, 256 (2010) 6060-6064.
- [23] Z. Grabarek, J. Gergely, Zero-length crosslinking procedure with the use of active esters, *Anal. Biochem.*, 185 (1990) 131-135.
- [24] A.J. Bard, L.R. Faulkner, *Electrochemical Methods: Fundamentals and Applications*, 2 ed., John Wiley & Sons Inc., New York, 2001.
- [25] Q. Zhao, D.P. Zhan, H.Y. Ma, M.Q. Zhang, Y.F. Zhao, P. Jing, Z.W. Zhu, X.H. Wan, Y.H. Shao, Q.K. Zhuang, Direct proteins electrochemistry based on ionic liquid mediated carbon nanotube modified glassy carbon electrode, *Front. Biosci.*, 10 (2005) 326-334.
- [26] H. Tao, W.Z. Wei, X.D. Zeng, X.Y. Liu, X.J. Zhang, Y.M. Zhang, Electrocatalytic oxidation and determination of estradiol using an electrode modified with carbon nanotubes and an ionic liquid, *Microchim. Acta*, 166 (2009) 53-59.
- [27] M. Tunckol, J. Durand, P. Serp, Carbon nanomaterial-ionic liquid hybrids, *Carbon*, 50 (2012) 4303-4334.
- [28] E. Laviron, General expression of the linear potential sweep voltammogram in the case of diffusionless electrochemical systems, *J. Electroanal. Chem.*, 101 (1979) 19-28.
- [29] L.T. Wang, Y. Zhang, Y.L. Du, D.B. Lu, Y.Z. Zhang, C.M. Wang, Simultaneous determination of catechol and hydroquinone based on poly (diallyldimethylammonium chloride) functionalized graphene-modified glassy carbon electrode, *J. Solid State Electrochem.*, 16 (2012) 1323-1331.
- [30] D. Kertesz, R. Zito, Mushroom polyphenol oxidase I. Purification and general properties, *Biochimica Et Biophysica Acta*, 96 (1965) 447-462.
- [31] Z.J. Liu, B.H. Liu, J.L. Kong, J.Q. Deng, Probing trace phenols based on mediator-free alumina sol-gel derived tyrosinase biosensor, *Anal. Chem.*, 72 (2000) 4707-4712.
- [32] Y.Y. Tan, J.Q. Kan, S.Q. Li, Amperometric biosensor for catechol using electrochemical template process, *Sens. Actuator B-Chem.*, 152 (2011) 285-291.
- [33] H.L. Qi, C.X. Zhang, Simultaneous determination of hydroquinone and catechol at a glassy carbon electrode modified with multiwall carbon nanotubes, *Electroanalysis*, 17 (2005) 832-838.

- [34] M.F. Chen, X. Li, X.Y. Ma, Selective determination of catechol in wastewater at silver doped polyglycine modified film electrode, *Int. J. Electrochem. Sci.*, 7 (2012) 2616-2622.
- [35] P. Dantoni, S.H.P. Serrano, A.M. Oliveira-Brett, I.G.R. Gutz, Flow-injection determination of catechol with a new tyrosinase/DNA biosensor, *Anal. Chim. Acta*, 366 (1998) 137-145.
- [36] Rajesh, W. Takashima, K. Kaneto, Amperometric phenol biosensor based on covalent immobilization of tyrosinase onto an electrochemically prepared novel copolymer poly (N-3-aminopropyl pyrrole-co-pyrrole) film, *Sens. Actuator B-Chem.*, 102 (2004) 271-277.
- [37] R. Solna, S. Sapelnikova, P. Skladal, M. Winther-Nielsen, C. Carlsson, J. Emneus, T. Ruzgas, Multienzyme electrochemical array sensor for determination of phenols and pesticides, *Talanta*, 65 (2005) 349-357.
- [38] H.B. Yildiz, J. Castillo, D.A. Guschin, L. Toppare, W. Schuhmann, Phenol biosensor based on electrochemically controlled integration of tyrosinase in a redox polymer, *Microchim. Acta*, 159 (2007) 27-34.
- [39] S. Tembe, S. Inamdar, S. Haram, M. Karve, S.F. D'Souza, Electrochemical biosensor for catechol using agarose-guar gum entrapped tyrosinase, *J. Biotechnol.*, 128 (2007) 80-85.
- [40] F. Kheiri, R.E. Sabzi, E. Jannatdoust, H. Sedghi, Acetone extracted propolis as a novel membrane and its application in phenol biosensors: the case of catechol, *J. Solid State Electrochem.*, 15 (2011) 2593-2599.
- [41] B. Perez-Lopez, A. Merkoci, Magnetic nanoparticles modified with carbon nanotubes for electrocatalytic magnetoswitchable biosensing applications, *Adv. Funct. Mater.*, 21 (2011) 255-260.
- [42] R.X. Han, L. Cui, S.Y. Ai, H.S. Yin, X.G. Liu, Y.Y. Qiu, Amperometric biosensor based on tyrosinase immobilized in hydrotalcite-like compounds film for the determination of polyphenols, *J. Solid State Electrochem.*, 16 (2012) 449-456.
- [43] X.P. Ji, X.R. Li, N. Wang, R.X. Ni, X.H. Liu, H.A. Xiong, Attachment of tyrosinase on mixed self-assembled monolayers for the construction of electrochemical biosensor, *Chin. Chem. Lett.*, 21 (2010) 1239-1242.
- [44] E. Burestedt, A. Narvaez, T. Ruzgas, L. Gorton, J. Emneus, E. Dominguez, G. MarkoVarga, Rate-limiting steps of tyrosinase-modified electrodes for the detection of catechol, *Anal. Chem.*, 68 (1996) 1605-1611.
- [45] B. Serra, S. Jimenez, M.L. Mena, A.J. Reviejo, J.M. Pingarron, Composite electrochemical biosensors: a comparison of three different electrode matrices for the construction of amperometric tyrosinase biosensors, *Biosens. Bioelectron.*, 17 (2002) 217-226.
- [46] S. Campuzano, B. Serra, M. Pedrero, F.J.M. de Villena, J.M. Pingarron, Amperometric flow-injection determination of phenolic compounds at self-assembled monolayer-based tyrosinase biosensors, *Anal. Chim. Acta*, 494 (2003) 187-197.
- [47] S. Kiralp, L. Toppare, Y. Yagci, Immobilization of polyphenol oxidase in conducting copolymers and determination of phenolic compounds in wines with enzyme electrodes, *Int. J. Biol. Macromol.*, 33 (2003) 37-41.
- [48] R.S. Brown, K.B. Male, J.H.T. Luong, A substrate recycling assay for phenolic-compounds using tyrosinase and NADH, *Anal. Biochem.*, 222 (1994) 131-139.
- [49] J.C. Espin, M. Morales, P.A. Garcia-Ruiz, J. Tudela, F. Garcia-Canovas, Improvement of a continuous spectrophotometric method for determining the monophenolase and diphenolase activities of mushroom polyphenol oxidase, *J. Agric. Food Chem.*, 45 (1997) 1084-1090.

[50] J.L. Smith, R.C. Krueger, Separation and purification of phenolases of common mushroom, *J. Biol. Chem.*, 237 (1962) 1121-1128.

[51] R.L. Anderson, *Practical Statistics for Analytical Chemists*, Van Nostrand Reinhold, New York, 1987.

Accepted Manuscript

Biographies

Fernando Campanhã Vicentini received the MS degree from the University of São Paulo, São Carlos, SP, Brazil in 2009, and Ph.D. degree from the Federal University of São Carlos, São Carlos, SP, Brazil in 2013. His research interests include the study of new electrode materials, carbon nanotubes, metallic nanoparticles and development of electrochemical sensors and biosensors.

Bruno Campos Janegitz received the MS degree from the Federal University of São Carlos, São Carlos, SP, Brazil in 2009, and Ph.D. degree in the same University, in 2012. At present, he is a postdoctoral researcher at the Physics Institute of São Carlos, University of São Paulo, São Carlos, SP, Brazil. His research interests include electroanalytical chemistry, nanostructured electrode materials and modified electrode surfaces, electrochemical sensors and biosensors.

Christopher Brett is a professor of chemistry at the University of Coimbra, Portugal. His research interests include new nanostructured electrode materials and modified electrode surfaces, electrochemical sensors and biosensors, electroactive polymers, corrosion and its inhibition and applications of electrochemistry in the environmental, food and pharmaceutical areas.

Orlando Fatibello-Filho received his PhD degree in Analytical Chemistry from São Paulo University and postdoctorate in 1989 from the University of New Orleans, USA. Currently, he is a full professor of Analytical Chemistry in the Department of Chemistry at the Federal University of São Carlos, Brazil. His research interests consist in the development of analytical procedures employing chemical sensors, biosensors, solid-

phase reactors and flow-injection systems and their application to the determination of analytes in pharmaceutical formulations, environmental and food samples.

Accepted Manuscript

Figure Captions

Fig. 1. Scheme of the reaction of IL, EDC and NHS with the MWCNT and the enzyme Tyr.

Fig. 2. SEM images of IL-MWCNT-DHP (A) and Tyr-IL-MWCNT-DHP (B) on the surface of the GCE.

Fig. 3. CVs of Tyr-MWCNT-DHP/GCE (A, dashed line) and Tyr-IL-MWCNT-DHP/GCE (B, solid line) after 30 cycles in a 1.0×10^{-4} mol L⁻¹ catechol / 0.1 mol L⁻¹ phosphate buffer solution (pH 7.0) at scan rate 100 mV s⁻¹.

Fig. 4. CVs of the Tyr-IL-MWCNT-DHP/GCE in a 1.0×10^{-4} mol L⁻¹ catechol / 0.1 mol L⁻¹ phosphate buffer solution, from pH 5.5 to 8.0. Scan rate 100 mV s⁻¹. Inset A: Influence of pH on the cathodic peak current. Inset B: dependence of $E^{0'}$ of Tyr versus pH.

Fig. 5. Schematic representation of the reduction of *o*-quinone produced in the enzymatic reaction catalysed by Tyr in the presence of oxygen on the Tyr-IL-MWCNT-DHP/GCE biosensor.

Fig. 6. LSVs obtained with the Tyr-IL-MWCNT-DHP/GCE biosensor in a 0.1 mol L⁻¹ phosphate buffer solution (pH 7.0) containing different concentrations of catechol: (a) 4.9×10^{-6} , (b) 2.2×10^{-5} , (c) 4.7×10^{-5} , (d) 9.8×10^{-5} , (e) 2.4×10^{-4} , (f) 4.7×10^{-4} , (g) 6.9×10^{-4} , (h) 9.0×10^{-4} (i) 1.1×10^{-3} mol L⁻¹. Inset: Analytical curve.

Table 1 Comparison of figures of merit obtained using the proposed biosensor and other tyrosinase biosensors for the determination of catechol.

Electrode	Linear range ($\mu\text{mol L}^{-1}$)	Detection Limit ($\mu\text{mol L}^{-1}$)	Sensitivity ($\text{mA mol}^{-1} \text{L}$)	
Tyr-DNA/CP	1.0 – 50	1.0	–	Shelf
Tyr-PAPCP/ITO	1.6 – 140	1.2	3.5	80% rema
Tyr/SPPtE	–	1.7	–	50-60% afte
Tyr-Oscomplex-functionalized/Pt	–	0.01	6.1	
Tyr-Agarose-guar gum/GCE	60 – 800	6.0	–	Shelf
Tyr-MWCNT-PPy/GCE	3.0 – 50	0.67	8.0	85% rema
Tyr/MWCNT/AuNPs/AEP/Au	1.0 – 500	0.8	150	80% rema
Tyr-MWCNT-MNP/SPE	10 – 80	7.6	4.8	Shelf
Tyr-MWCNT	0.2 – 10	0.2	226	72% rema
Tyr-PO ₄ -PPy/Pt	10 – 120	0.84	47	80% rema
Tyr-PANI/Pt	5.0 – 140	0.05	–	90% rema
Tyr-HTLc/GCE	3.0 – 300	0.1	–	72% rema
Tyr-IL-MWCNT-DHP/GCE	4.9 – 1100	0.58	32.8	95% rema

CP: Carbon paste; PAPCP: Poly (*N*-3-aminopropyl pyrrole-co-pyrrole); ITO: indium-tin-oxide; SPPtE: Screen-printed Pt electrode; Os: Osmium; Pt: Platinum electrode; PPy: Polypyrrole; AuNPs: Gold nanoparticles; AEP: Acetone-extracted propolis; Au: Gold electrode; MNP: Magnetic nanoparticles; PANI: polyaniline; HTLc: Mg–Al–CO₃ hydrotalcite-like.

Table 2 K_M^{app} values of different Tyr biosensors for catechol.

Biosensor	$K_M^{\text{app}}/\text{mol L}^{-1}$	Reference
Tyr-MWCNT-MNP/SPE	1.8×10^{-4}	[41]
Tyr-SAMs/Au	1.8×10^{-4}	[43]
Tyr-IL-MWCNT-DHP/GCE	1.9×10^{-4}	This work
Tyr/GE	1.9×10^{-4}	[44]
Tyr/RVC-ER	2.0×10^{-4}	[45]
Free Tyr	2.8×10^{-4}	[48]
Tyr-MPA-SAMs/Au	3.3×10^{-4}	[46]
Free Tyr	4.4×10^{-4}	[49]
Free Tyr	4.0×10^{-3}	[50]
Tyr-PPy/Pt	1.0×10^{-1}	[47]
Tyr-PPy-MM/Pt	2.0×10^{-1}	[47]

SPE: Screen printed electrode; MNP: Magnetic nanoparticles; Au: Gold electrode; SAMs: Self-assembled monolayers; GE: Graphite electrodes; RVC-ER: Reticulated vitreous carbon-epoxy-resin; MPA: 3-mercaptopropionic acid; PPy: Polypyrrole; MM: menthyl monomer.

Table 3 Determination of catechol in water samples by LSV using the Tyr-IL-MWCNT-DHP/GCE biosensor and spectrophotometric method .

Samples	Catechol (10^{-6} mol L $^{-1}$)		
	Reference method*	LSV method	Relative error**
A	50.9 ± 0.2	51.2 ± 0.4	+0.6
B	49.0 ± 0.4	53.8 ± 0.6	+9.8
C	49.1 ± 0.2	51.0 ± 0.3	+3.9
D	51.4 ± 0.6	49.2 ± 0.5	-4.3

* spectrophotometric method - Average of 3 measurements.

** [(proposed method – reference method) × 100] /reference method.

Figure 1 colored

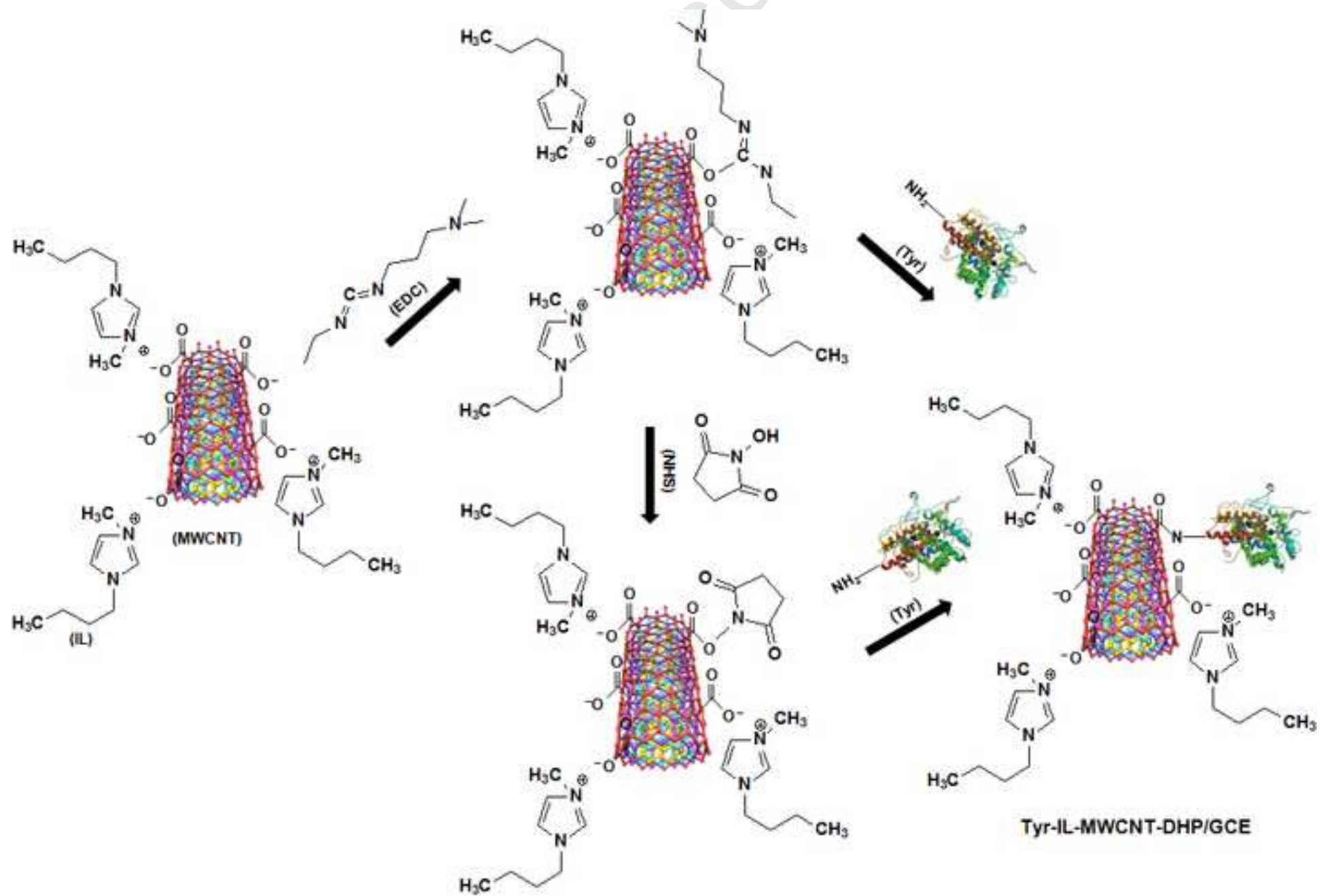
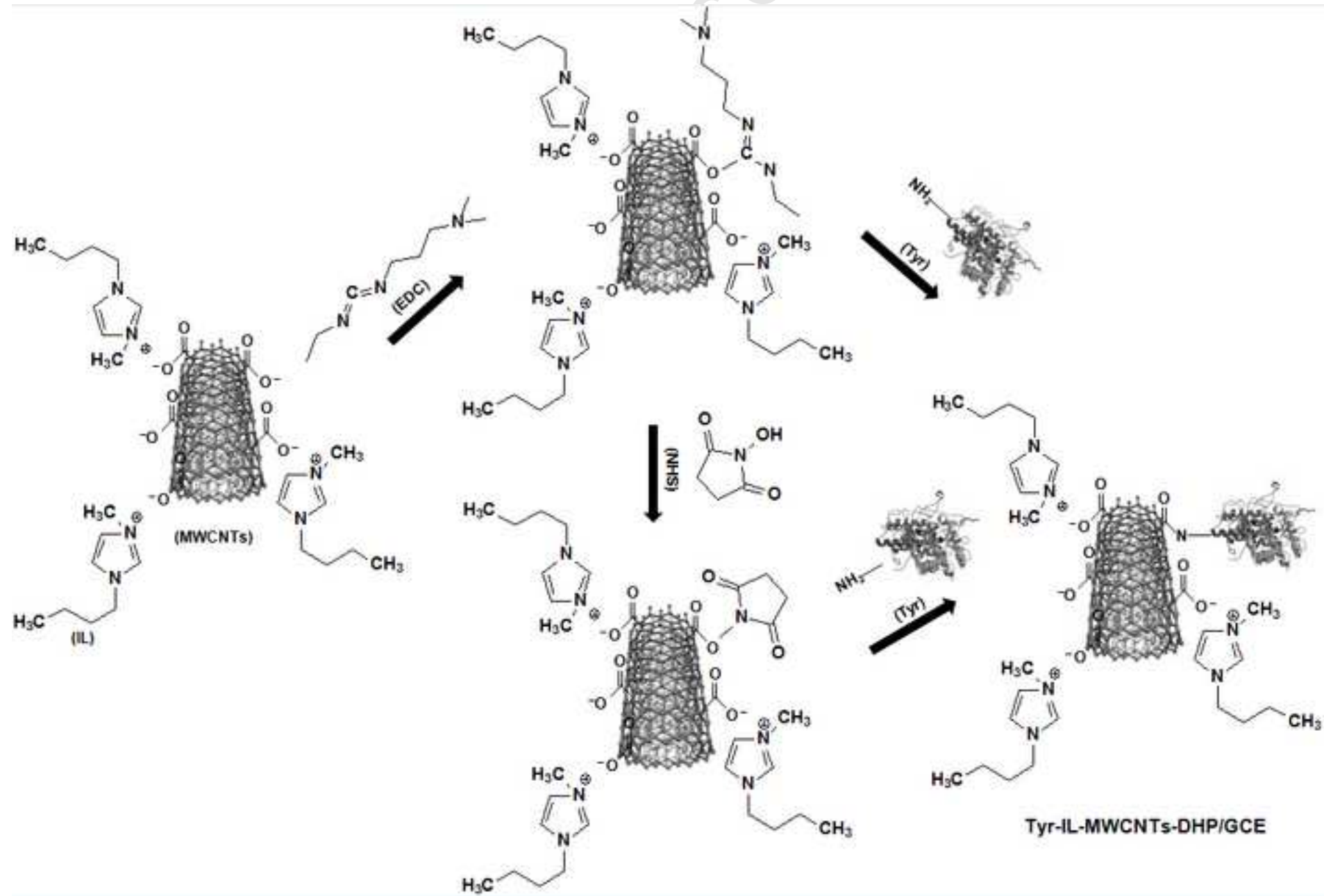


Figure 1 gray



Manuscript

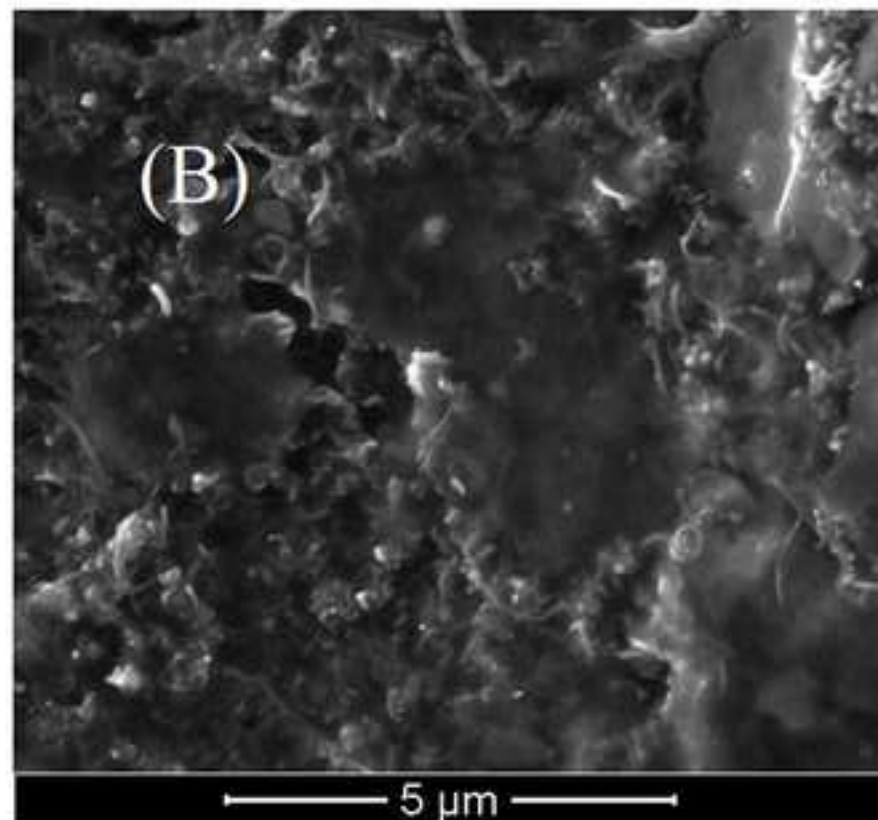
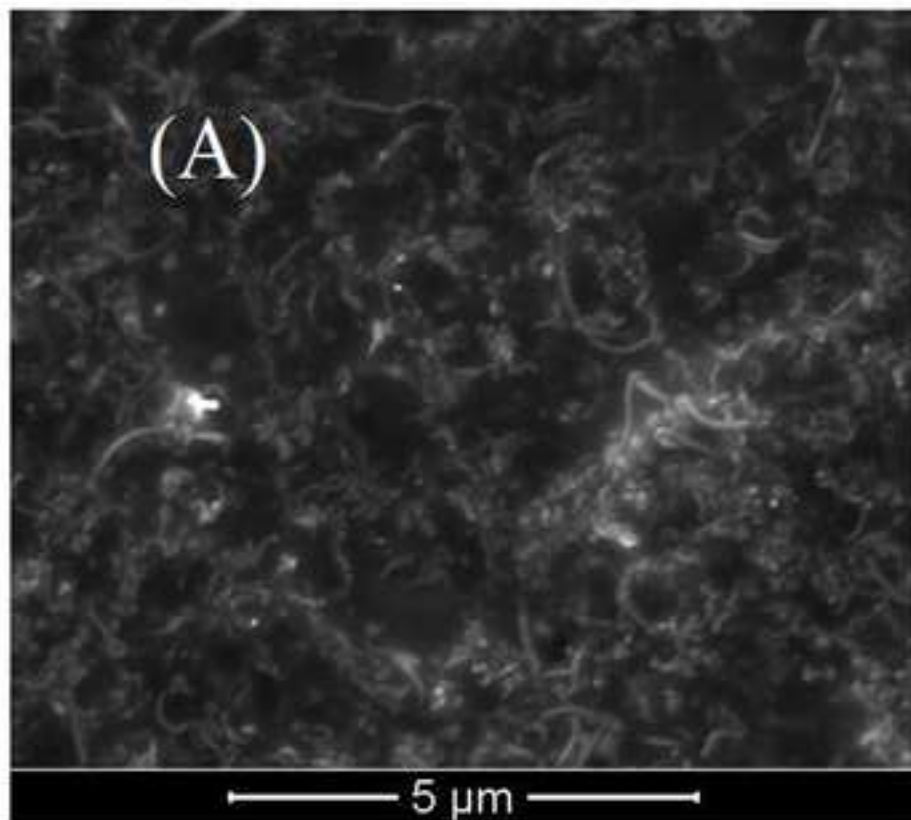


Figure 3

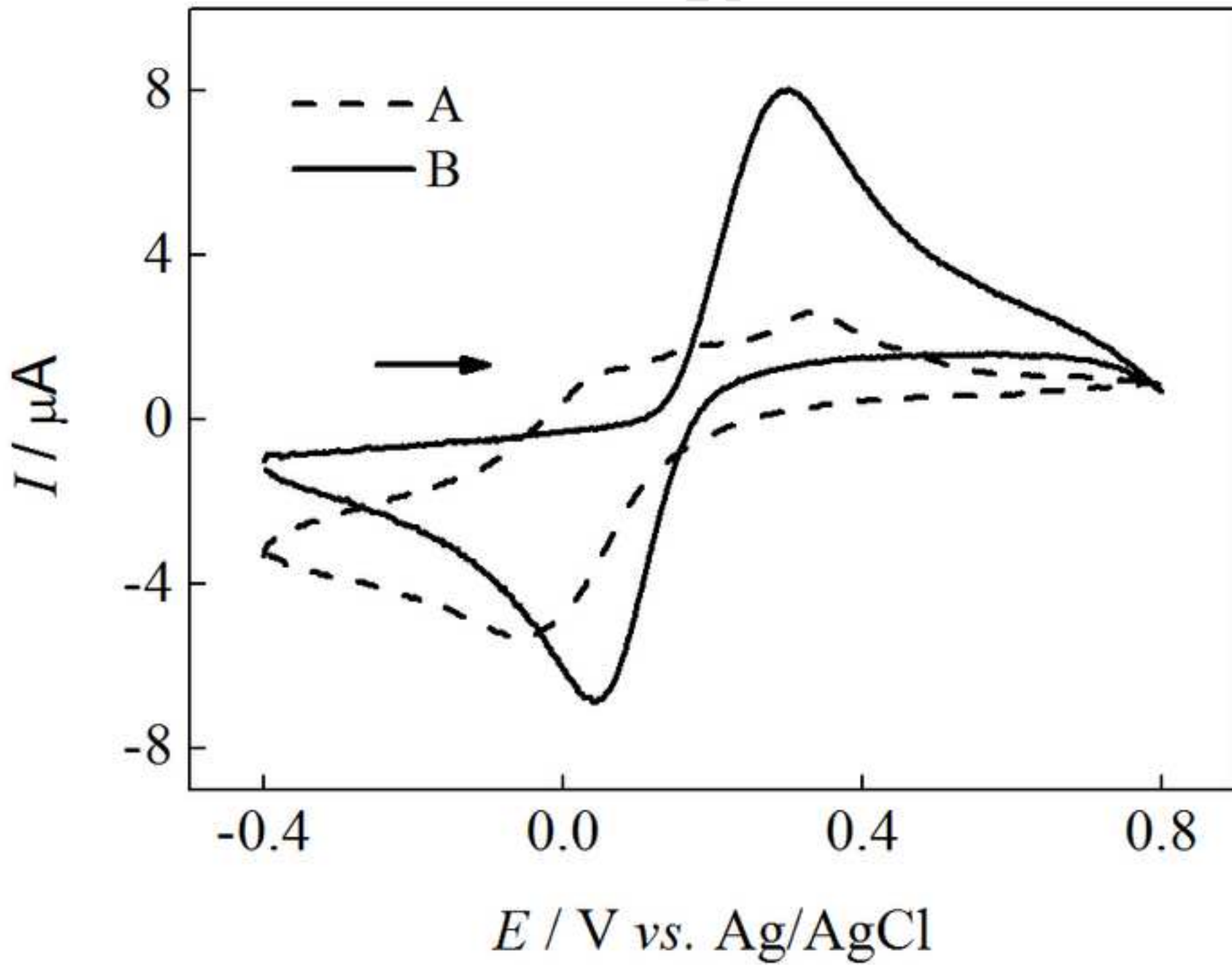
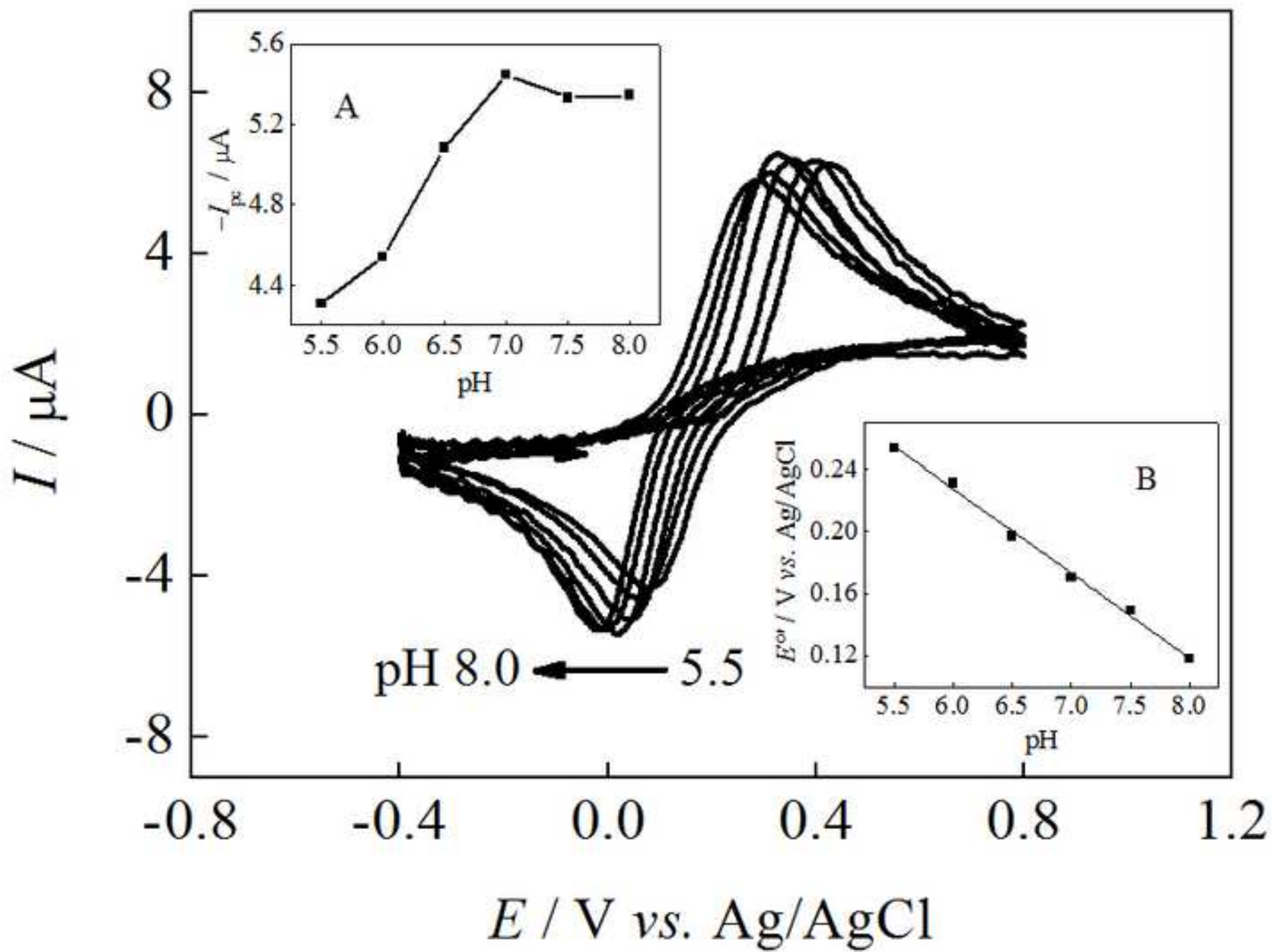


Figure 4



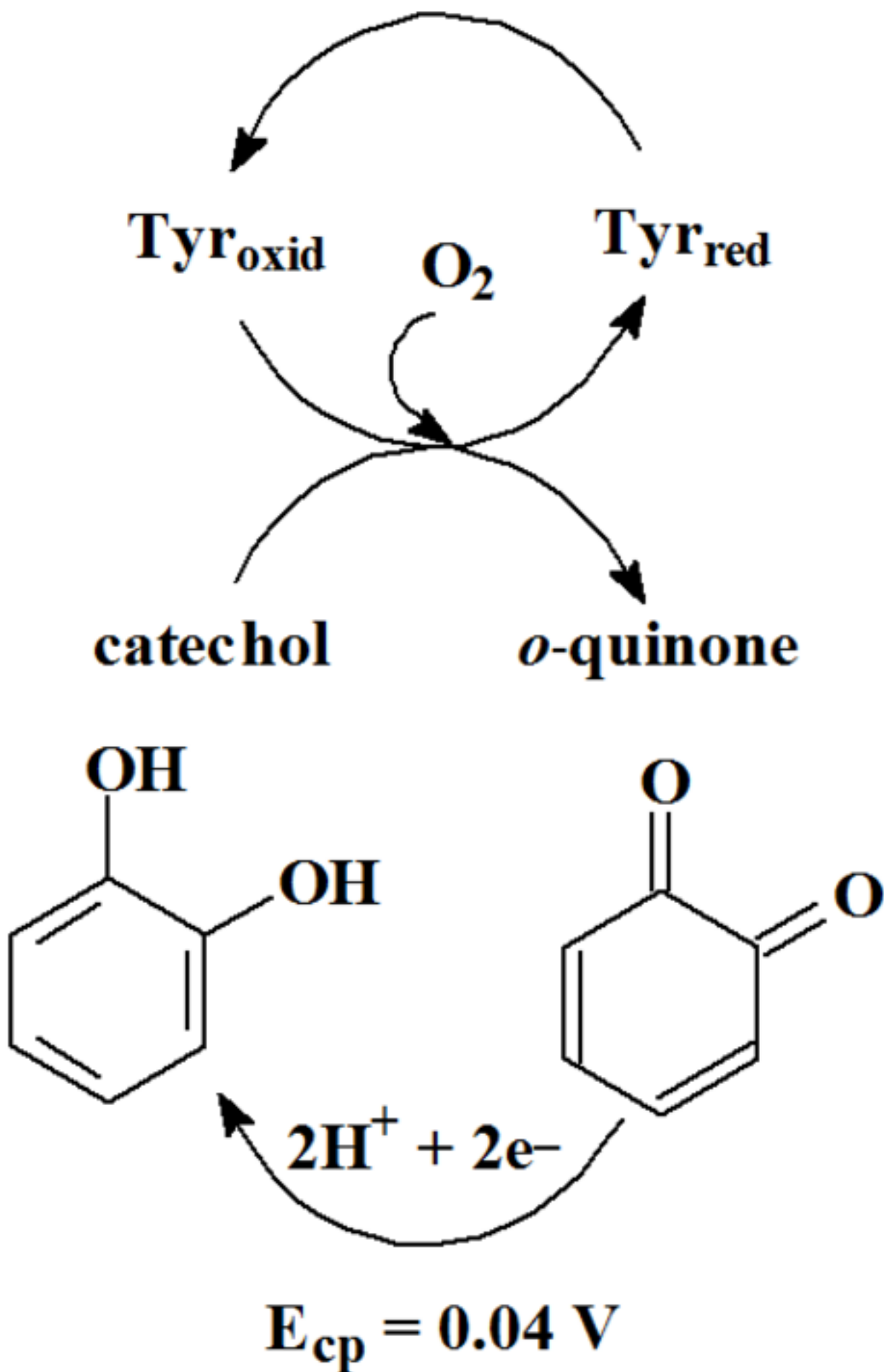


Figure 6

